Cell PRESS
Neuron
Article

Control of Synaptic Plasticity and Memory via Suppression of Poly(A)-Binding Protein

Arkady Khoutorsky,[1] Akiko Yanagiya,[1,7] Christos G. Gkogkas,[1,7] Marc R. Fabian,[2] Masha Prager-Khoutorsky,[3] Ruifeng Cao,[1] Karine Gamache,[4] Frederic Bouthiette,[5] Armen Parsyan,[1] Robert E. Sorge,[6] Jeffrey S. Mogil,[6] Karim Nader,[4] Jean-Claude Lacaille,[5,*] and Nahum Sonenberg[1,*]

[1]Department of Biochemistry and Rosalind and Morris Goodman Cancer Research Centre, McGill University, Montréal, QC H3A 1A3, Canada
[2]Lady Davis Institute for Medical Research, Jewish General Hospital, Department of Oncology, McGill University, Montreal, QC H3T 1E2, Canada
[3]Center for Research in Neuroscience, Montréal General Hospital, McGill University, Montréal, QC, H3G 1A4 Canada
[4]Department of Psychology, McGill University, Montréal, QC H3A 1B1, Canada
[5]Groupe de Recherche sur le Système Nerveux Central and Département de Physiologie, Université de Montréal, Montréal, QC H3C 3J7, Canada
[6]Department of Psychology and Alan Edwards Centre for Research on Pain, McGill University, Montréal, QC H3A 1B1, Canada
[7]These authors contributed equally to this work
*Correspondence: nahum.sonenberg@mcgill.ca (N.S.), jean-claude.lacaille@umontreal.ca (J.-C.L.)
http://dx.doi.org/10.1016/j.neuron.2013.02.025

SUMMARY

Control of protein synthesis is critical for synaptic plasticity and memory formation. However, the molecular mechanisms linking neuronal activity to activation of mRNA translation are not fully understood. Here, we report that the translational repressor poly(A)-binding protein (PABP)-interacting protein 2A (PAIP2A), an inhibitor of PABP, is rapidly proteolyzed by calpains in stimulated neurons and following training for contextual memory. *Paip2a* knockout mice exhibit a lowered threshold for the induction of sustained long-term potentiation and an enhancement of long-term memory after weak training. Translation of *CaMKII*α mRNA is enhanced in *Paip2a*$^{-/-}$ slices upon tetanic stimulation and in the hippocampus of *Paip2a*$^{-/-}$ mice following contextual fear learning. We demonstrate that activity-dependent degradation of PAIP2A relieves translational inhibition of memory-related genes through PABP reactivation and conclude that PAIP2A is a pivotal translational regulator of synaptic plasticity and memory.

INTRODUCTION

The formation of long-lasting memory requires de novo synthesis of mRNA and proteins and is blocked by inhibitors of transcription or translation, whereas short-term memory relies on the modification of pre-existing proteins and is not affected by such inhibitors. Similarly, long-term potentiation (LTP), a cellular model for learning and memory, is dependent on transcription and translation for its late phase (late LTP; L-LTP), which lasts for many hours, while its early phase (early LTP; E-LTP) lasts 1–2 hr and is translation independent (Kandel, 2001; Silva, 2003).

Neuronal mRNA translation is tightly regulated by synaptic activity (Banerjee et al., 2009; Kelleher et al., 2004a; Richter and Klann, 2009; Sutton and Schuman, 2006). Synaptic stimulation activates several signaling pathways that control the translation of a subset of mRNAs via 5′- and 3′-untranslated region (UTR)-dependent mechanisms. All nuclear-transcribed eukaryotic mRNAs contain at their 5′ end a m^{7}GpppN structure (where m is a methyl group and N is any nucleotide) termed the "cap," and most mRNAs contain a 3′-terminal poly(A) tail. Ribosome recruitment to the mRNA is facilitated by the eukaryotic initiation factor 4F (eIF4F), which binds the 5′ cap. eIF4F is a multisubunit complex composed of the following: (1) eIF4E, the cap-binding subunit; (2) eIF4G, a large scaffolding protein; and, (3) eIF4A, an RNA helicase. The assembly of the eIF4F complex is controlled by the mechanistic/mammalian target of rapamycin (mTOR) pathway, which, in neurons, is stimulated by activity and plays a key role in synaptic plasticity and memory formation (Hoeffer et al., 2008; Kelleher et al., 2004b). Translation is also enhanced by the poly(A) tail through the poly(A)-binding protein (PABP) (Derry et al., 2006). PABP binds simultaneously to the poly(A) tail and eIF4G, resulting in the mRNA circularization, which facilitates translation initiation (Gray et al., 2000; Kahvejian et al., 2001). Translation is also regulated by PABP-interacting proteins (PAIPs), which function to control PABP activity. PAIP1 stimulates translation via its interactions with PABP, eIF4A, and eIF3 (Martineau et al., 2008). Conversely, PAIP2 strongly inhibits translation by competing with the poly(A) tail and eIF4G for binding to PABP, thus reducing PABP-poly(A) tail and PABP-eIF4G interactions (Karim et al., 2006; Khaleghpour et al., 2001). Two homologs of PAIP2 exist in mammals: PAIP2A and PAIP2B. No functional or mechanistic differences between PAIP2A and PAIP2B have been reported; however, the tissue distributions of PAIP2A and PAIP2B differ at both the mRNA and protein levels in mice (Berlanga et al., 2006). PAIP2A is expressed in the brain at much higher levels than PAIP2B (Yanagiya et al., 2010).

Given the important role of PABP in translational control (Derry et al., 2006), its presence in dendrites (Muddashetty et al., 2002),

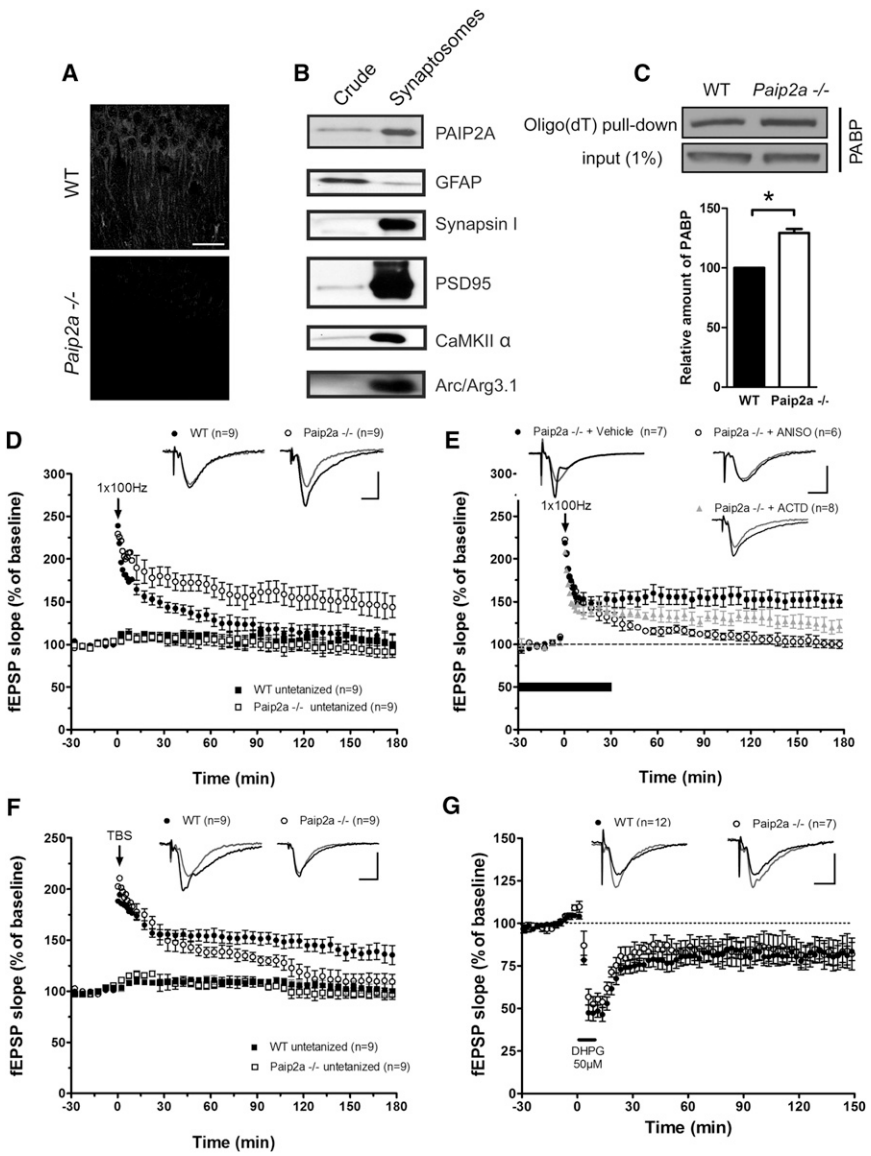

Figure 1. The Threshold for Induction of L-LTP Is Lowered in Slices from *Paip2a*$^{-/-}$ Mice

(A) Confocal images of hippocampal pyramidal neurons immunostained for PAIP2A (CA1) in sections from WT and *Paip2a*$^{-/-}$ mice. Scale bar represents 20 μm.

(B) Synaptosomes were prepared from mouse hippocampi (crude: total hippocampal lysate).

(C) Oligo(dT) pulldown assay was used to isolate mRNA from WT and *Paip2a*$^{-/-}$ brains. The amount of PABP associated with mRNA was assessed by western blot analysis. For quantification, intensity of each band was normalized to the level of mRNA in each sample (n = 3).

(D) 1HFS (1 s, 100 Hz) induces E-LTP in WT (filled circles) but L-LTP in *Paip2a*$^{-/-}$ slices (open circles).

(E) Sustained L-LTP in *Paip2a*$^{-/-}$ slices is suppressed by treatment with anisomycin (open circles, at 180 min, $p < 0.01$) or actinomycin D (triangles, at 180 min, $p < 0.05$) applied 30 min before tetanization for 60 min (indicated by black horizontal bar).

(F) L-LTP induced by TBS is impaired in slices from *Paip2a*$^{-/-}$ mice (at 180 min, $p < 0.05$).

(G) For induction of LTD, DHPG (50 μM) was applied for 10 min. fEPSPs were depressed similarly in slices from WT and *Paip2a*$^{-/-}$ mice. Horizontal scale bars represent 5 ms; vertical scale bars represent 1 mV. Data are presented as mean ± SEM. *$p < 0.05$.

See also Figures S1 and S2.

and the pervasive paradigm of activating gene expression by removing inhibitory constraints (Abel et al., 1998; Shimizu et al., 2007), we reasoned that PAIP2A might play a role in controlling synaptic plasticity and memory. Here, we show that calcium-activated proteases, calpains, rapidly proteolyze PAIP2A in cultured neurons after stimulation with NMDA or with KCl-induced depolarization. Moreover, PAIP2A is rapidly degraded in hippocampal slices following tetanic stimulation and in the dorsal hippocampus after training for contextual memory. Hippocampal slices from *Paip2a*$^{-/-}$ mice exhibit a lowered threshold for induction of L-LTP, and *Paip2a*$^{-/-}$ mice exhibit enhanced spatial memory after weak training. The translation of *CaMKIIα* mRNA, which is essential for memory formation, is enhanced in *Paip2a*$^{-/-}$ mice, demonstrating that translation of this mRNA is constrained by PAIP2A. Thus, our data demonstrate that PAIP2A functions as a negative regulator of synaptic plasticity and memory by suppressing PABP activity in the mammalian brain.

RESULTS

Paip2a$^{-/-}$ Hippocampal Slices Exhibit a Lowered Threshold for the Induction of Protein Synthesis-Dependent L-LTP

PAIP2A is expressed in the cell body and dendrites of pyramidal cells in the CA1 region of the mouse hippocampus (Figure 1A) and is present in the synaptosomal fraction prepared from adult hippocampus (Figure 1B). We investigated the role of PAIP2A in synaptic plasticity and memory using *Paip2a*$^{-/-}$ mice (Yanagiya et al., 2010). PAIP2A was not detected in the brain of *Paip2a*$^{-/-}$ mice, as determined by western blotting (Figure S1A available online). A statistically significant increase in the levels of PABP bound to mRNA in *Paip2a*$^{-/-}$ mice, as compared to wild-type (WT), was evident (29.3% ± 3.4%, $p < 0.05$; Figure 1C), consistent with the previously established inhibition of the PABP-poly(A) tail interaction by PAIP2A (Khaleghpour et al., 2001). We did not detect any gross morphological abnormalities in the brain of *Paip2a* knockout (KO) mice as assessed by Nissl staining (Figures S1B and S1C) or by immunohistochemistry of brain sections for synaptophysin, a marker of synapses (Figure S1D). In addition, the number of VGLUT (presynaptic marker) and PSD-95 (postsynaptic marker) puncta in stratum radiatum of CA1 hippocampus did not differ between WT and *Paip2a*$^{-/-}$ mice

(Figures S1E and S1F), and neither did spine density (Figure S1G) or dendritic arbor (Figure S2A).

Since PAIP2A is a translational repressor, we hypothesized that brain slices from *Paip2a*$^{-/-}$ mice should manifest enhanced protein synthesis-dependent LTP. A single high-frequency stimulation (1HFS) of the Schaffer collateral-CA1 synapses elicited transient short-lasting potentiation (E-LTP) of field excitatory postsynaptic potentials (fEPSPs) in slices from WT animals, which decays after 1.5 hr and does not require new protein synthesis (Figure 1D). In striking contrast, in slices from *Paip2a*$^{-/-}$ littermates, 1HFS elicited LTP that persisted for at least 3 hr after induction. The transition from transient to sustained potentiation after 1HFS in *Paip2a*$^{-/-}$ slices was protein synthesis dependent, as treatment with anisomycin, an inhibitor of protein synthesis, during tetanization abolished L-LTP in *Paip2a*$^{-/-}$ slices (Figure 1E), similarly to the inhibition of theta-burst stimulation (TBS)-induced L-LTP in WT slices (Figure S2B). Actinomycin-D, a transcription inhibitor, also reduced L-LTP in *Paip2a*$^{-/-}$ slices but to a lesser extent than anisomycin (Figure 1E). It is important to note that basal synaptic transmission in *Paip2a*$^{-/-}$ slices was not different from that in WT slices as evidenced by the input-output relation of fEPSPs and paired-pulse facilitation (Figures S2C and S2D, respectively), demonstrating that these effects are not due to changes in basal synaptic transmission. Next, we examined the effect of *Paip2a* ablation on L-LTP induced with TBS. Whereas in WT slices TBS induced persistent potentiation, in *Paip2a*$^{-/-}$ slices L-LTP was impaired (Figures 1F). General protein synthesis, as assessed by puromycin incorporation into the newly synthesized polypeptide chains (SUnSET method) (Bhattacharya et al., 2012; Hoeffer et al., 2011), was increased after TBS in stratum radiatum at CA1 area in WT and *Paip2a*$^{-/-}$ slices. However, the increase was bigger in *Paip2a*$^{-/-}$ slices (Figure S2E), indicating an association of excessive stimulation of mRNA translation and impaired L-LTP after TBS in *Paip2a*$^{-/-}$ slices (see Discussion). Long-term depression (LTD) elicited by application of DHPG (3,5-dihydroxyphenylglycine, an mGluR1/5 agonist) or by low-frequency stimulation (LFS) was not altered in *Paip2a*$^{-/-}$ slices (Figures 1G and S2F, respectively). Taken together, these results show that the threshold for the induction of protein synthesis-dependent L-LTP is lowered in *Paip2a*$^{-/-}$ slices. In contrast, stronger stimulation (TBS) leads to L-LTP impairment, while LTD is not affected.

Enhanced Spatial Memory in *Paip2a*$^{-/-}$ Mice

Based on the electrophysiological results, we predicted that *Paip2a*$^{-/-}$ mice would exhibit enhanced learning and memory after weak training. We investigated this using the hidden version of the Morris water maze task (MWM), a hippocampal-dependent task for spatial learning and memory (Morris et al., 1982). *Paip2a*$^{-/-}$ and WT littermates were trained with a weak training protocol that consisted of only a single training trial per day to find a submerged platform, in contrast to the standard protocol of three trials per day (Costa-Mattioli et al., 2005, 2007). Overall, the swim latencies were not different between WT and *Paip2a*$^{-/-}$ mice over 6 days of training; $F(1, 14) = 2.5$, $p = 0.136$, repeated-measures ANOVA. However, on the third training day, *Paip2a*$^{-/-}$ mice reached the hidden platform significantly faster (WT: 57.13 ± 7.31 s; *Paip2a*$^{-/-}$: 37.9 ± 4.90 s, $p < 0.05$, Student's t test) than WT mice (Figure 2A), indicating faster learning since there were no differences in swimming speed (WT: 15.93 ± 1.52 cm/s; *Paip2a*$^{-/-}$: 17.13 ± 0.73 cm/s, $p > 0.05$), thigmotaxis (swimming near the pool wall; WT: 44.88% ± 4.42%; *Paip2a*$^{-/-}$: 41.88% ± 5.38%, $p > 0.05$), or escape latency in the visible version of MWM (WT: 11.38 ± 2.12 s; *Paip2a*$^{-/-}$: 12.25 ± 3.05 s, $p > 0.05$). A probe test performed 24 hr after 3 days of training confirmed superior spatial memory in *Paip2a*$^{-/-}$ mice. WT mice demonstrated no preference for the quadrant where the platform was located during the training sessions (target quadrant), whereas *Paip2a*$^{-/-}$ mice displayed a clear preference for the target quadrant and platform location (Figures 2B and 2C, respectively), spent significantly more time in the target quadrant (Figure 2B), and crossed the platform location significantly more than WT mice (Figure 2C). In the probe test, after 6 days of training, both groups demonstrated similar quadrant occupancy and platform crossing (Figures 2D and 2E, respectively).

Next, we used an object-location memory task to assess spatial long-term memory (LTM) of *Paip2a*$^{-/-}$ mice. This is a hippocampus-dependent task that is based on the tendency of mice to spend more time exploring an object that has been relocated (Assini et al., 2009). *Paip2a*$^{-/-}$ mice performed better in this task than WT littermates (Figure 2F). We found no differences between the two genotypes in the novel object recognition task (Figure 2G), which examines recognition memory. Taken together, our data indicate that *Paip2a*$^{-/-}$ mice display enhanced spatial learning and memory as compared to WT littermates.

Altered Long-Term Contextual Memory in *Paip2a*$^{-/-}$ Mice

To study memory consolidation, we used contextual fear conditioning, a hippocampal-dependent task that engenders robust protein synthesis-dependent long-term memory for a training context following a single session of pairing the context to a foot shock (Kelleher et al., 2004b). Since a weak stimulation (1HFS) in *Paip2a*$^{-/-}$ slices elicited L-LTP, we first examined the effect of training using a weak experimental paradigm (single 0.3 mA foot shock for 1 s). Long-term contextual fear memory was assessed 24 hr later by reintroducing the mice to the training context. *Paip2a*$^{-/-}$ mice froze significantly more than WT littermates (WT: 32.6% ± 3.1%; *Paip2a*$^{-/-}$: 46.76% ± 4.0%, $p < 0.05$; Figure 2H), indicating an enhancement of long-term memory. No difference in freezing between the two groups was found 1 hr after the training, demonstrating that the acquisition of the task was intact (Figure S3A). To rule out possible nonspecific effects of nociceptive sensitivity or motor ability, we examined pain sensation in the radiant heat paw withdrawal (Figure S3B) and von Frey tests (Figure S3C) and motor coordination in the rotarod test (Figure S3D). No differences between *Paip2a*$^{-/-}$ and WT mice in these assays were observed.

Next, we assessed long-term memory of *Paip2a*$^{-/-}$ mice using pairing of context to a strong foot shock (strong training, two foot shocks of 0.5 mA for 2 s separated by 1 min). *Paip2a*$^{-/-}$ mice exhibited reduced freezing 24 hr after strong training, thus demonstrating an impairment of long-term contextual memory (Figure 2I). Freezing 1 hr after strong training was not altered,

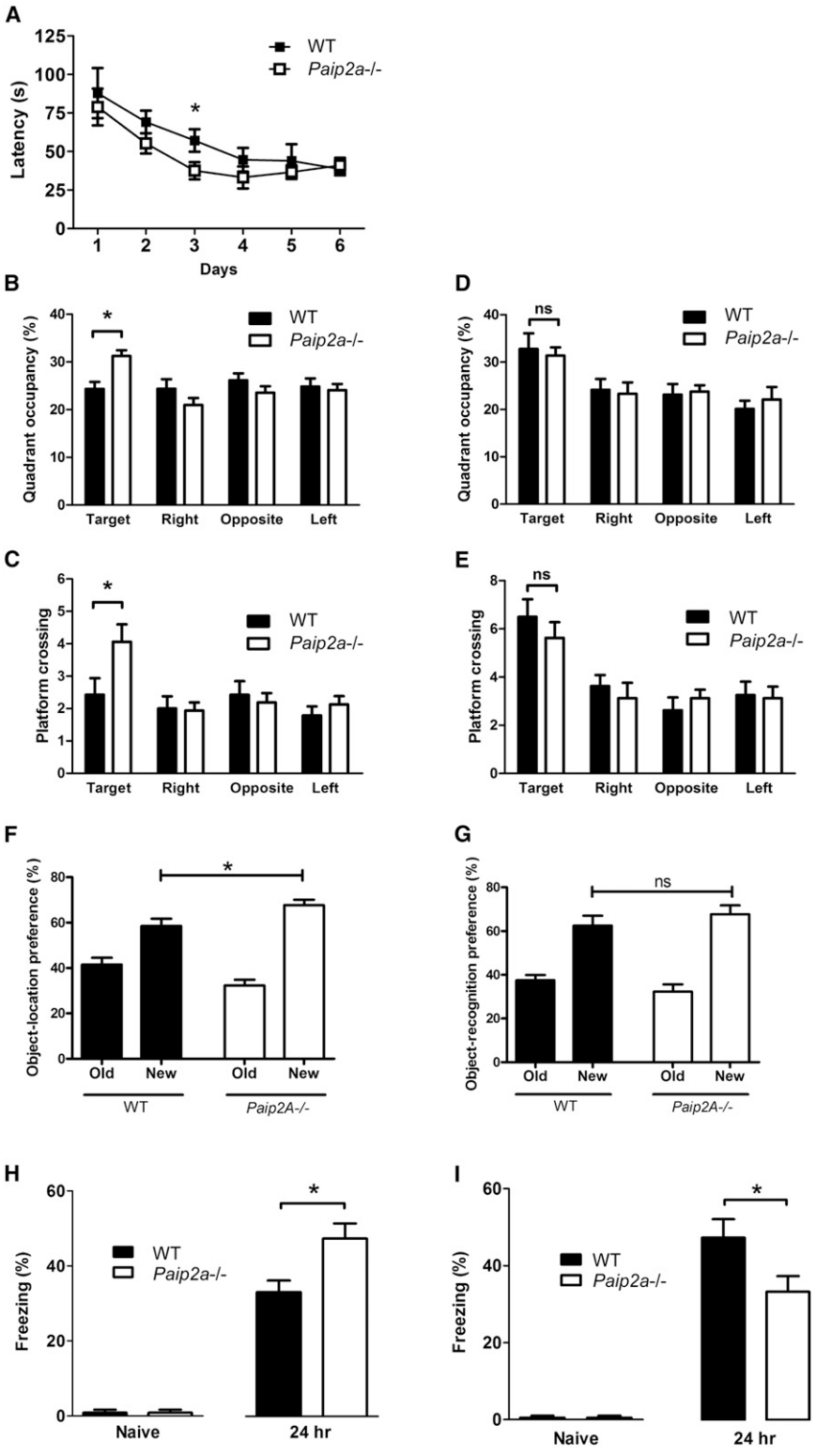

Figure 2. Altered Spatial Memory in *Paip2a*$^{-/-}$ Mice

Spatial memory of *Paip2a*$^{-/-}$ mice was assessed in the hidden platform version of the MWM using a weak training protocol that consisted of one training session per day.

(A–E) In (A), latency to find the submerged platform is plotted during the training phase of the task. On the third day, the *Paip2a*$^{-/-}$ mice demonstrated significantly lower latency than WT mice ($n = 12$ for each group, $p < 0.05$), suggesting a faster rate of learning. A probe test, performed 24 hr after the third training day showed increased quadrant occupancy (B) and platform crossing (C) in *Paip2a*$^{-/-}$ mice compared to WT ($p < 0.05$ for both parameters). Target quadrant occupancy (D) and platform crossing (E) were not different between *Paip2a*$^{-/-}$ and WT mice on the probe test performed 24 hr after the sixth training day.

(F and G) In (F), *Paip2a*$^{-/-}$ mice exhibit an enhanced long-term object location memory at 24 hr after training ($n = 9$ for each group, $p < 0.05$), while in (G), long-term object recognition memory is not altered ($n = 8$ for WT, $n = 9$ for *Paip2a*$^{-/-}$).

(H and I) Long-term contextual fear memory in *Paip2a*$^{-/-}$ mice is enhanced after weak training and impaired after strong training. *Paip2a*$^{-/-}$ and their WT littermates were trained in a contextual fear conditioning task with either a weak protocol (one 1 s foot shock, 0.3 mA) or with a strong protocol (two foot shocks of 2 s spaced by 30 s, 0.5 mA). Freezing behavior was measured during the first 2 min before shocking (naive) and 24 hr after training when the mice were reintroduced to the training context. *Paip2a*$^{-/-}$ mice froze more 24 hr after weak training (H; $n = 10$ for each group, $p < 0.05$) and less after strong training (I; $n = 10$ for each group, $p < 0.05$). Data are presented as mean ± SEM. *$p < 0.05$.

See also Figures S3 and S4.

demonstrating intact acquisition (Figure S3E). Extinction of contextual fear memories in *Paip2a*$^{-/-}$ mice was impaired as well (Figure S3F). We also assessed cued associative memory of *Paip2a*$^{-/-}$ mice using auditory fear conditioning, an amygdala-dependent task that leads to association of the tone with the foot shock, with weak and strong training protocols (Costa-Mattioli et al., 2005). No difference in freezing in response to the tone was detected 24 hr after training (Figures S3G and S3H), demonstrating that long-term auditory fear memory is not altered in *Paip2a*$^{-/-}$ mice. Taken together, these results show that hippocampus-dependent long-term memory is enhanced in *Paip2a*$^{-/-}$ mice as compared to their WT littermates following weak training and is impaired after strong training. It is important to note that analogous effects of weak versus strong stimulation were exhibited in electrophysiological experiments when 1HFS (weak)

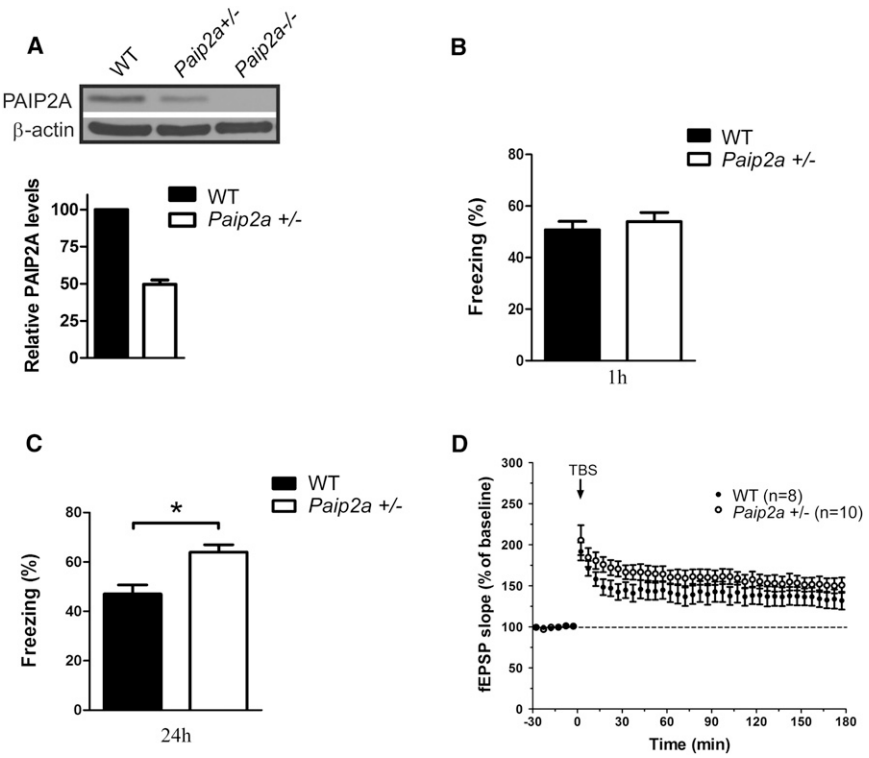

Figure 3. Long-Term Contextual Memory Is Enhanced in *Paip2a* Heterozygous Mice after Strong Training

(A–C) In (A), PAIP2A is reduced in *Paip2a* heterozygous mice (+/−). $Paip2a^{+/-}$ mice were subjected to contextual fear conditioning using strong foot shock, and freezing behavior was measured 1 hr (B) and 24 hr (C) later in the same context. Long-term contextual fear memory (24 hr) was enhanced in $Paip2a^{+/-}$ mice as compared to WT littermates ($n = 8$ for each group, $p < 0.05$).

(D) L-LTP in slices from *Paip2a* heterozygous mice was not altered after TBS (at 180 min, $p > 0.05$). Data are presented as mean ± SEM. *$p < 0.05$.

induced long-lasting L-LTP and TBS (strong) resulted in L-LTP impairment.

An attractive explanation for the impairment of long-term contextual memory after strong training in $Paip2a^{-/-}$ mice is excessive activity-induced translation in the absence of PAIP2A. It is conceivable that partial reduction of PAIP2A, as in $Paip2a^{+/-}$ mice, might have a smaller effect on translation and thus lead to a salubrious effect on memory. Reduction in the PAIP2A protein levels in $Paip2a^{+/-}$ mice was confirmed by western blotting (Figure 3A). It is striking that, while similar freezing was observed 1 hr after strong contextual training, it was enhanced 24 hr after training in $Paip2a^{+/-}$ relative to WT mice (Figures 3B and 3C). These data are consistent with the idea that complete removal of PAIP2A might cause memory impairment via excessive translation in response to strong training. In accordance with these results, L-LTP elicited by TBS was not impaired in $Paip2a^{+/-}$ relative to WT hippocampal slices (Figure 3D).

Because adult neurogenesis contributes to fear memory extinction (Pan et al., 2012), which is impaired in $Paip2a^{-/-}$ mice, we examined neurogenesis in WT, $Paip2a^{-/-}$, and $Paip2a^{+/-}$ mice. Progenitor cell proliferation within the subgranular zone of the dentate gyrus was assessed using systemic injection of BrdU followed by immunostaining or by staining for Ki-67, a marker of proliferating progenitor cells. It is surprising that the number of BrdU- and Ki-67-positive cells was reduced in $Paip2a^{-/-}$ but not in $Paip2a^{+/-}$ mice as compared to WT mice (Figure S4A), suggesting that impaired memory extinction in $Paip2a^{-/-}$ mice might result from reduced adult neurogenesis.

We also examined the memory phenotype of $Paip2b^{-/-}$ mice, although PAIP2B expression in the brain is lower than PAIP2A (Berlanga et al., 2006). No differences were found in contextual fear conditioning task between $Paip2b^{-/-}$ mice and their WT littermates 1 hr and 24 hr after training (Figures S4B and S4C, respectively), suggesting that PAIP2B is not involved in translational regulation of learning and memory.

Activity-Dependent Degradation of PAIP2A

Next, it was pertinent to determine whether PAIP2A is controlled in an activity-dependent manner. No phosphorylation of PAIP2A has been reported. However, PAIP2A levels are homeostatically controlled by proteasome-mediated degradation upon PABP depletion in cell cultures (Yoshida et al., 2006). Therefore, cultured neurons were depolarized with KCl for 5 min to study the effect on PAIP2A levels. PAIP2A protein levels decreased to 69.6% ± 3.3% of baseline 1 min after KCl-induced depolarization and were further reduced to 59.3% ± 4.0% after 10 min. PAIP2A levels returned to normal after 30 min (Figure 4A). Similarly, activation of NMDA receptors with NMDA resulted in the reduction of PAIP2A to 71.8% ± 2.2% of prestimulation levels (Figure 4B). We reasoned that the rapid downregulation of PAIP2A is mediated by proteolytic activity. To identify the protease responsible for PAIP2A degradation, we used inhibitors of calpain (calpeptin and calpain inhibitor I/III), proteasome (lactacystin), and caspase-3 (caspase-3 inhibitor), since these proteases are activated following synaptic stimulation (Bingol and Schuman, 2006; Chan and Mattson, 1999; Vanderklish et al., 1995, 2000) and are implicated in synaptic plasticity and memory (Bingol and Sheng, 2011; Li et al., 2010; Lynch et al., 2007). Calpain inhibitors rescued PAIP2A degradation, while proteasome and caspase-3 inhibitors failed to do so (Figures 4B and 4C). Consistent with these results, strong tetanic stimulation (using TBS) in acute hippocampal slices led to a decrease (55.25% ± 5.99% of control levels) in PAIP2A levels in the CA1 region, which was blocked by the calpain inhibitor (Figure 4D). Weak stimulation (using 1HFS) had a smaller effect on PAIP2A levels (76.58% ± 4.73% of control levels). Thus, calpain-mediated PAIP2A proteolysis is induced by synaptic activity in situ.

To determine whether PAIP2A levels also decrease in vivo in response to activity, mice were trained in the contextual fear-conditioning task and lysates from dorsal hippocampi were

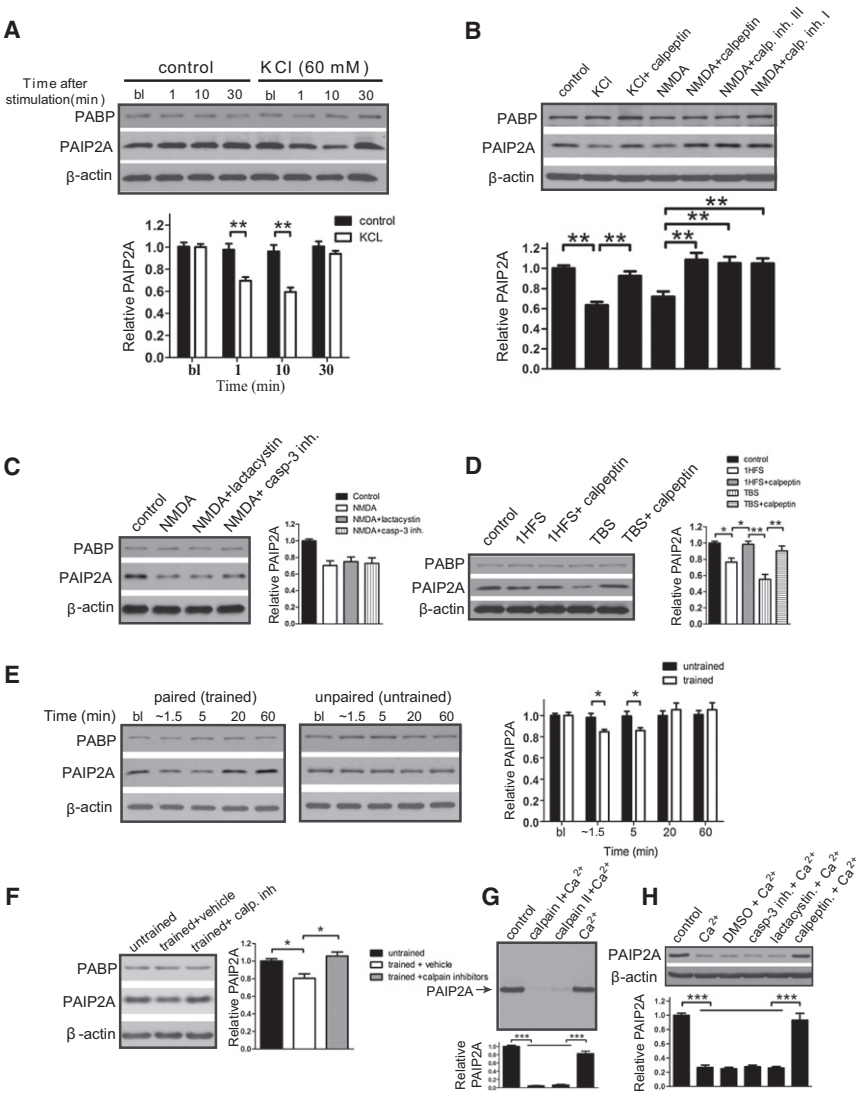

Figure 4. PAIP2A Is Proteolyzed by Calpain in an Activity-Dependent Manner

(A) Dissociated cortical cultured neurons (18–21 days in vitro) were depolarized with KCl (60 mM) for 5 min, and PAIP2A levels were assessed at different time points after stimulation by western blot analysis. Quantification of PAIP2A band intensity normalized to corresponding β-actin is shown at the summary graph below (n = 3). Sham-treated control neurons show no decrease in PAIP2A (control, n = 3). bl, baseline.

(B) Neurons pretreated for 20 min with calpain inhibitors calpeptin (10 μM) or calpain inhibitor I or III (20 μM) were stimulated for 5 min with either KCl (60 mM) or NMDA (50 μM). PAIP2A levels were decreased 5 min after KCl and NMDA stimulation. Calpain inhibitors prevented KCl- and NMDA-induced PAIP2A downregulation. Each column in the histogram represents corresponding PAIP2A band intensity normalized to β-actin (n = 4).

(C) NMDA-induced PAIP2A decrease is not prevented by proteasome inhibitor lactacystin (10 μM) or caspase 3 inhibitor (10 μM).

(D) TBS leads to PAIP2A decrease in microdissected CA1 area of acute hippocampal slices. Calpeptin (10 μM) applied 30 min before TBS prevented PAIP2A decrease. Right, quantification of PAIP2A band intensity (n = 4).

(E) WT mice were subjected to contextual fear conditioning using a weak training protocol (trained); the mice were sacrificed at different time points after the training protocol, and the dorsal hippocampi were dissected and subjected to western blot analysis (n = 3 per time point). Control mice received a foot shock immediately after being placed in the training context and were returned to their home cage after the shocking (untrained). Histogram on the right shows quantification of PAIP2A band intensity normalized to β-actin. bl, baseline.

(F) Calpain inhibition prevents PAIP2A downregulation after behavioral training. Calpain inhibitors cocktail or vehicle solution was bilaterally infused into the hippocampi of cannulated rats 45 min before fear conditioning training. Three minutes after training, rats were euthanized, their brains were snap frozen in liquid nitrogen, and hippocampal tissue surrounding the cannula tip was dissected and subjected to western blot analysis. Right, quantification of PAIP2A band intensity normalized to β-actin (n = 6 per group).

(G) PAIP2A is protealyzed by both calpain I and calpain II in vitro. PAIP2A, immunoprecipitated from the mouse brain, was incubated with purified calpain I or II in the presence of calcium (4 mM). After 1 hr at 37°C, the amount of PAIP2A was assessed by western blot analysis.

(H) PAIP2A degradation is calcium dependent. Brain lysates were incubated for 3 hr at 4°C at different conditions: calpeptin, 10 μM; lactacystin, 10 μM; caspase-3 inhibitor, 10 μM; calcium, 4 mM. Data are presented as mean ± SEM. *p < 0.05. **p < 0.01.

See also Figure S5.

subjected to western blot analysis. Control mice received the equivalent foot shock without pairing to the context. PAIP2A was reduced to 84.64% ± 2.2% of basal level at ~1.5 min after the end of training (2.5 min after foot shock) and was significantly lower than in untrained mice (untrained: 98.15% ± 3.7%, p < 0.05; Figure 4E). PAIP2A returned to prestimulation levels 20 min after training. To examine whether downregulation of PAIP2A in vivo is mediated by calpains, we infused a mixture of calpain inhibitors into the dorsal hippocampus of bilaterally cannulated rats before subjecting them to the contextual fear conditioning training. PAIP2A levels decreased in vehicle-treated rats to 80.3% ± 5% relative to untrained animals but did not change when calpain inhibitors were added (Figure 4F), demonstrating that PAIP2A degradation is mediated by calpain. In accordance with previous studies documenting a critical role for calpain in synaptic plasticity and memory formation (Lynch and Baudry, 1984; Shimizu et al., 2007), we also found that inhibiting calpain activity impaired long-term contextual fear memory without affecting short-term memory (Figure S5). To investigate calpain-mediated degradation in vitro, we treated immunoprecipitated PAIP2A from mouse brain with purified calpains I and II. PAIP2A levels decreased after 1 hr, showing that both calpain isoforms proteolyze PAIP2A (Figure 4G). Degradation of PAIP2A in brain lysates was calcium dependent (Figure 4H) and was

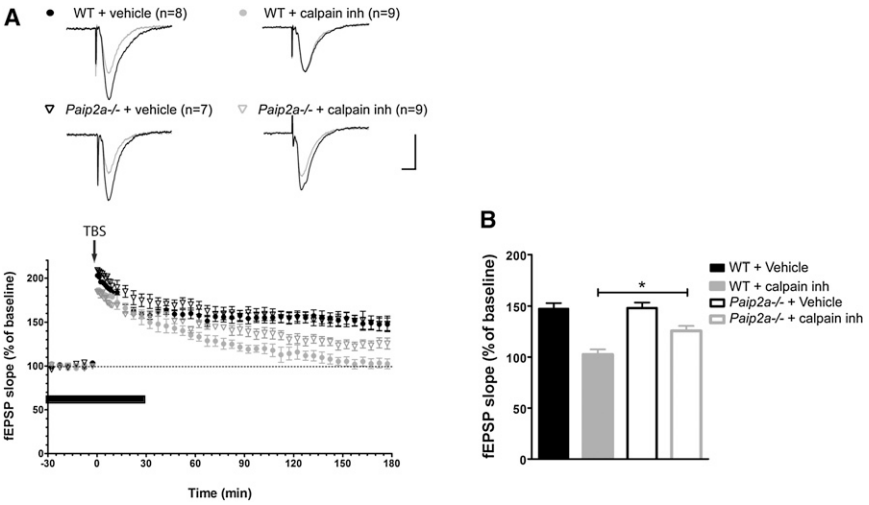

Figure 5. The Inhibitory Effect of Calpain Inhibitors on L-LTP Is Reduced in *Paip2a*$^{-/-}$ Slices

(A) L-LTP was induced in WT and *Paip2a*$^{-/-}$ slices in the presence and absence of calpain inhibitors (calpain inhibitor I, calpain inhibitor III, and calpeptin, 20 μM each). In *Paip2a*$^{-/-}$ slices, L-LTP was induced with 1HFS, while in WT slices, L-LTP was induced with TBS. In WT slices, calpain inhibitors blocked L-LTP, whereas in *Paip2a*$^{-/-}$ slices, the reduction of L-LTP was only partial.

(B) Summary bar graph showing differences in the induced L-LTP. fEPSP slopes were averaged over the last 15 min of the experiment. Horizontal scale bar represents 8 ms; vertical scale bar represents 0.4 mV. Data are presented as mean ± SEM. *$p < 0.05$.

prevented by calpain inhibitor but not by proteasome and caspase-3 inhibitors.

To examine the role of calpain-mediated PAIP2A degradation in L-LTP, we tested the effect of calpain inhibition on L-LTP in WT and *Paip2a*$^{-/-}$ hippocampal slices. In accordance with previous reports (del Cerro et al., 1990; Vanderklish et al., 1996), calpain inhibition abolished L-LTP in WT slices; however, in *Paip2a*$^{-/-}$ slices, calpain inhibitors only partially reduced L-LTP (Figure 5). These data suggest that, although degradation of PAIP2A by calpains is important for long-lasting potentiation, cleavage of other calpain targets also contributes to this process. Taken together, our data show that calpain-mediated PAIP2A degradation following synaptic activation and contextual learning plays an important role in hippocampal synaptic plasticity and memory formation.

Activity-Induced Translation of *CaMKIIα* mRNA Is Enhanced in *Paip2a*$^{-/-}$ Mice

CaMKIIα is essential for synaptic plasticity and learning (Frankland et al., 2001; Giese et al., 1998; Mayford et al., 1996b; Miller et al., 2002; Silva et al., 1992a, 1992b). *CaMKIIα* mRNA is highly expressed in dendrites (Burgin et al., 1990) and is translated locally upon stimulation via 5′ and 3′-UTR mRNA-dependent mechanisms (Aakalu et al., 2001; Banerjee et al., 2009; Gong et al., 2006; Huang et al., 2002; Mayford et al., 1996a; Ouyang et al., 1999). To investigate whether PAIP2A and PABP play a role in control of *CaMKIIα* mRNA translation, we examined basal and activity-dependent *CaMKIIα* expression in WT and *Paip2a*$^{-/-}$ mice. First, we examined protein levels of CaMKIIα and Arc (activity-regulated cytoskeleton-associated protein) in the hippocampus of WT and *Paip2a*$^{-/-}$ mice under basal conditions and found that they were not different (Figure 6A). Next, we assessed activity-induced expression of CaMKIIα and Arc proteins in *Paip2a*$^{-/-}$ mice. To this end, we trained WT and *Paip2a*$^{-/-}$ mice in a contextual fear conditioning task and measured protein levels of CaMKIIα and Arc in the dorsal hippocampus after 90 min. Consistent with previous studies (Lonergan et al., 2010), behavioral training upregulated Arc protein levels (Figure 6C). However, the increase in Arc was similar in WT and *Paip2a*$^{-/-}$ mice. It is striking that, although CaMKIIα did not increase significantly after training in WT mice, CaMKIIα protein levels were significantly higher in trained *Paip2a*$^{-/-}$ as compared to untrained *Paip2a*$^{-/-}$ mice (increase of CaMKIIα in WT: 20.7% ± 10.6%, $p > 0.05$; increase in *Paip2a*$^{-/-}$: 63.2% ± 12.8%, $p < 0.05$; Figures 6C and 6D). Thus, activity-induced CaMKIIα expression is markedly enhanced in the hippocampus of *Paip2a*$^{-/-}$ mice.

To determine whether the increase in CaMKIIα was the result of increased translation, extracts from dorsal hippocampi of *Paip2a*$^{-/-}$ and WT mice were fractionated on sucrose density gradients (Figure 6B), and the distribution of several mRNAs across these gradients was determined by quantitative real-time PCR (qRT-PCR) analysis. *CaMKIIα* mRNA shifted to the heavy polysome fractions after training in *Paip2a*$^{-/-}$ mice, indicative of enhanced translation (Figures 6E). In WT mice, a small and statistically not significant shift was observed (Figure 6E). We hypothesized that increased translation of *CaMKIIα* mRNA in *Paip2a*$^{-/-}$ mice after training is the result of increased availability of PABP because of the absence of PAIP2A, leading to augmented binding of PABP to the *CaMKIIα* mRNA poly(A) tail. To test this hypothesis, we measured the association of *CaMKIIα* mRNA with PABP in the hippocampus of WT and *Paip2a*$^{-/-}$ mice using a ribonucleoprotein immunoprecipitation (RIP) assay with PABP antibody. The association of PABP with *CaMKIIα* mRNAs was increased after contextual training in both groups. However, the increase was greater in *Paip2a*$^{-/-}$ mice as compared to WT mice (Figure 6F). Taken together, our data demonstrate that, while translation of *CaMKIIα* mRNA is not altered in *Paip2a*$^{-/-}$ mice under basal conditions, contextual training of *Paip2a*$^{-/-}$ mice leads to enhanced *CaMKIIα* mRNA translation. This is consistent with previous studies showing that the *CaMKIIα* mRNA contains two cytoplasmic polyadenylation elements (CPEs), binds the CPE binding protein, and undergoes NMDA- and experience-dependent elongation of poly(A) tail at synapses (Huang et al., 2002; Wu et al., 1998). Translational activation by newly formed poly(A)

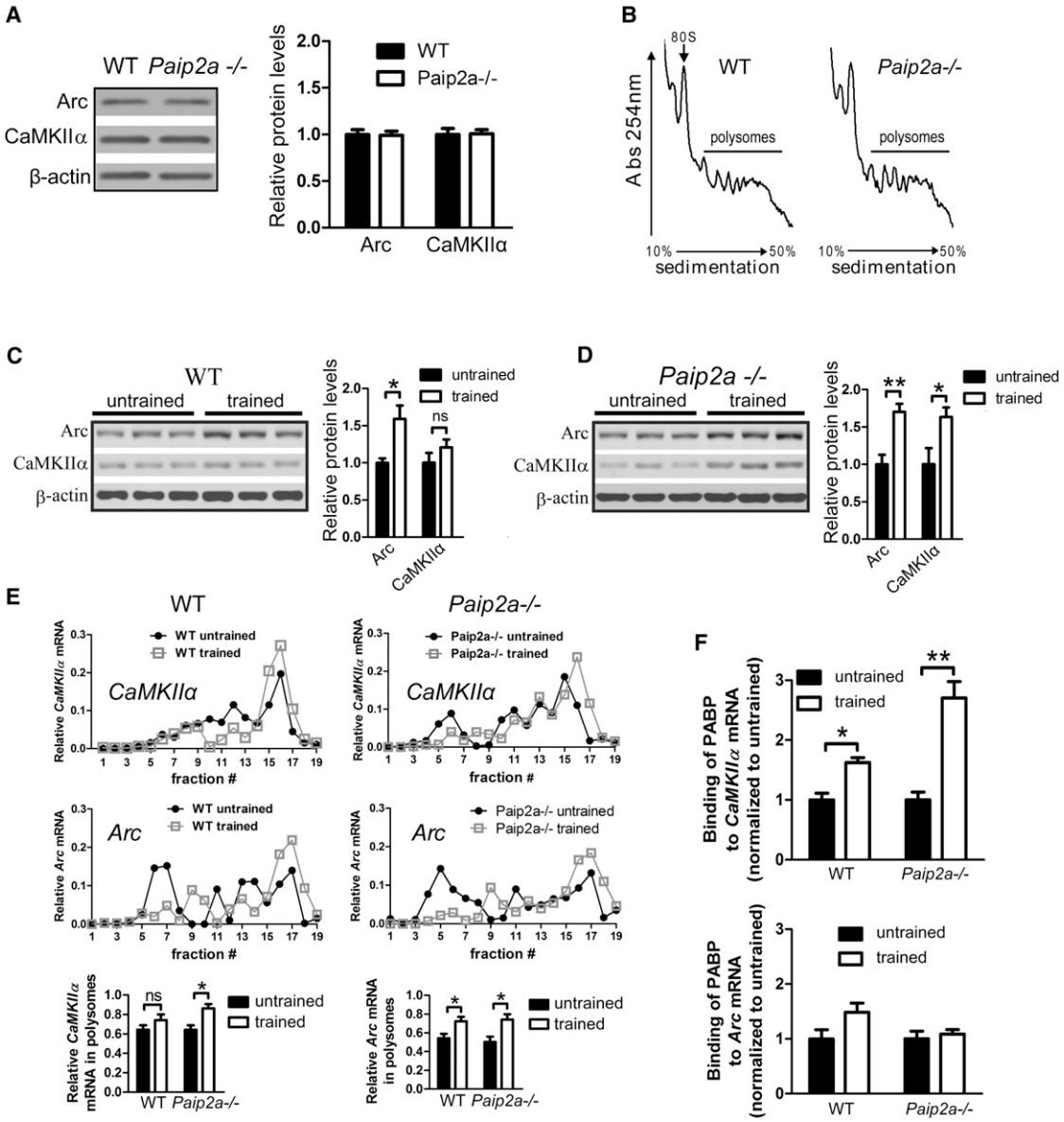

Figure 6. Activity-Induced Translation of *CaMKIIα* mRNA Is Enhanced in *Paip2a*$^{-/-}$ Mice

(A) No change in *Arc and CaMKIIα* protein levels in the hippocampus of *Paip2a*$^{-/-}$ mice under basal conditions.

(B–D) In (B), polysome profiling of dorsal hippocampus lysates from WT (left) and *Paip2a*$^{-/-}$ (right) mice is shown. WT and *Paip2a*$^{-/-}$ mice were trained in a contextual fear conditioning task with a strong training protocol. Control (untrained) mice received a foot shock only without pairing to the training context. Ninety minutes after training, the dorsal hippocampi were isolated and processed for western blot analysis. Whereas no significant increase in CaMKIIα levels was found in WT mice after training (C; n = 6 for each group), the expression of CaMKIIα was significantly increased in *Paip2a*$^{-/-}$ mice (D; n = 6 for each group). Behavioral training increased expression of Arc in a manner similar to that in WT and *Paip2a*$^{-/-}$ mice.

(E) Distribution of *Arc and CaMKIIα* mRNAs across sucrose gradient fractions prepared from dorsal hippocampus of untrained and trained WT (left) and *Paip2a*$^{-/-}$ (right) mice. Relative mRNA amounts in polysomal fractions are shown in the histogram below (n = 3 for each group). No differences in the levels of total *Arc* and *CaMKIIα* mRNAs were found between WT and *Paip2a*$^{-/-}$ mice (not shown).

(F) Binding of PABP to *CaMKIIα* (top) and *Arc* (bottom) mRNAs in dorsal hippocampus of untrained and trained WT and *Paip2a*$^{-/-}$ mice was assessed by RIP assay (n = 3). No differences in the protein levels of PABP or mRNA levels of *Arc* and *CaMKIIα* were detected prior to immunoprecipitation (input) in the samples from WT and *Paip2a*$^{-/-}$ hippocampus (not shown). Data are presented as mean ± SEM. *p < 0.05. **p < 0.01.

tail depends on PABP binding, which, in turn, is regulated by PAIP2A.

We next examined the enhancement of *CaMKIIα* mRNA translation in *Paip2a*$^{-/-}$ mice by using immunostaining. Previous studies reported that tetanic stimulation increases CaMKIIα levels in CA1 pyramidal cell dendrites of acute hippocampal slices as early as 5 min after the stimulation in a protein synthesis-dependent manner (Gong et al., 2006; Ouyang et al., 1999).

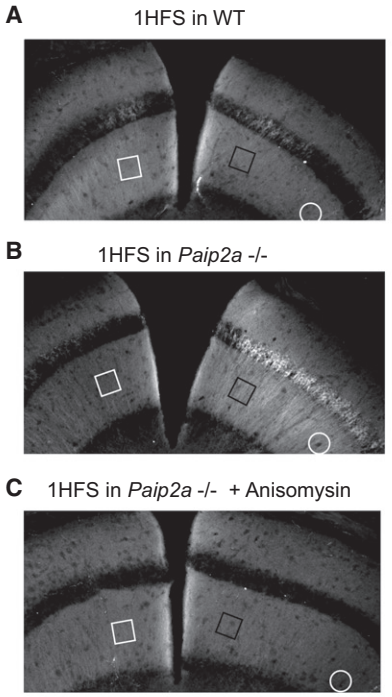

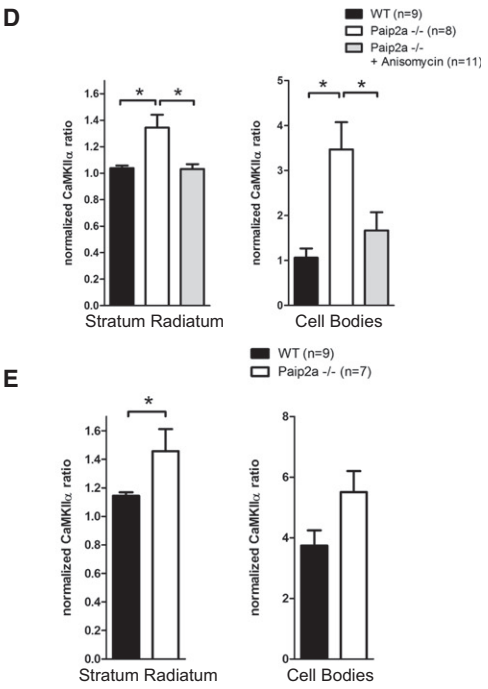

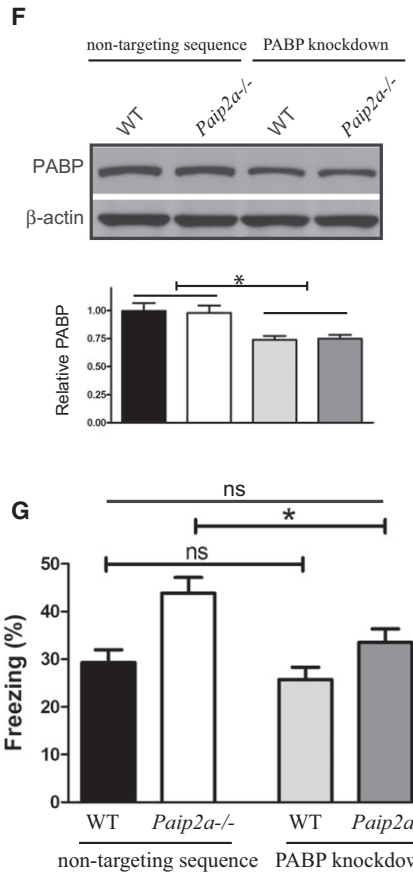

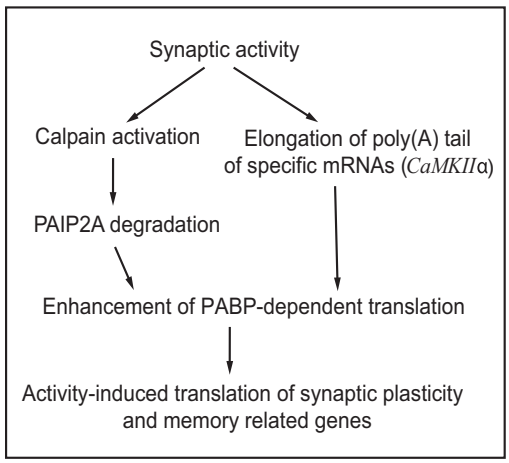

(legend on next page)

Tetanus-induced dendritic translation of CaMKIIα mRNA in CA1 pyramidal cells in acute hippocampal slices from WT and *Paip2a*$^{-/-}$ mice was examined. A surgical cut was made across the CA1 area perpendicularly to the pyramidal cell layer to separate tetanized and untetanized slice regions (Gong et al., 2006). Thirty minutes after tetanic stimulation, slices were fixed and processed for CaMKIIα fluorescent immunostaining, and the ratio of the CaMKIIα fluorescent signal from the dendritic area of the stimulated and the control sides was calculated. 1HFS induced no change in CaMKIIα amounts in WT slices (Figures 7A and 7D), but in *Paip2a*$^{-/-}$ slices, 1HFS led to a significant increase in CaMKIIα expression (WT: 3.8% ± 1.9%; *Paip2a*$^{-/-}$: 34.5% ± 9.7%, $p < 0.01$; Figures 7B and 7D). The increase in dendritic expression of CaMKIIα in *Paip2a*$^{-/-}$ slices was abolished when anisomycin was present during tetanization (Figures 7C and 7D), demonstrating that increased levels of CaMKIIα protein is due to upregulation of *CaMKIIα* mRNA translation. These results indicate that, as with L-LTP, the threshold for induction of dendritic *CaMKIIα* mRNA translation is lowered in *Paip2a*$^{-/-}$ slices. It is striking that TBS increased CaMKIIα levels to a greater degree in *Paip2a*$^{-/-}$ slices than in WT slices (WT: 14.5% ± 2.3%; *Paip2a*$^{-/-}$: 45.8% ± 15.4%, $p < 0.05$; Figure 7E), which supports in vivo results that demonstrate increased *CaMKIIα* mRNA translation following behavioral training.

To directly examine our model that greater availability of PABP in the absence of PAIP2A leads to memory enhancement, we knocked down PABP in WT and *Paip2a*$^{-/-}$ mice using intrahippocampal injection of lentiviruses expressing shRNA against *PABP* (Figure 7F). Reducing PABP levels in *Paip2a*$^{-/-}$ mice normalized the enhanced LTM in contextual fear conditioning task (Figure 7G), thus supporting our model that enhanced PABP activity contributes to the memory phenotype of *Paip2a*$^{-/-}$ mice.

DISCUSSION

Here we show a mechanism that controls mRNA translation in the mammalian brain through the regulation of PABP availability. This is accomplished by activity-induced degradation of PAIP2A, a protein that inhibits translation via binding to PABP to suppress its activity. This process is critical for synaptic plasticity, learning, and memory formation. According to our model, synaptic activity-induced calcium influx activates calpains that degrade PAIP2A (Figure 7H). Decreased PAIP2A levels, in turn, result in a larger pool of free PABP that stimulates translation through enhanced binding of PABP to mRNA poly(A) tail.

Translation of *CaMKIIα* mRNAs Is Regulated by PAIP2A

The poly(A) tail of *CaMKIIα* mRNA is elongated upon synaptic activity and visual experience (Huang et al., 2002; Wu et al., 1998). Consistent with this, we showed that contextual training is associated with increased PABP binding to *CaMKIIα* mRNA in the dorsal hippocampus of WT mice. Since PABP availability is increased in *Paip2a*$^{-/-}$ mice, binding of PABP to *CaMKIIα* mRNA was augmented, thereby leading to enhanced translation of *CaMKIIα* mRNA upon activity. Similarly, activity-induced degradation of PAIP2A in WT mice increases PABP availability for binding poly(A) tails and stimulates translation of *CaMKIIα* mRNA. Thus, dendritic polyadenylation and PAIP2A degradation control in concert CaMKIIα expression in an activity-dependent manner.

Activity-Dependent Proteolysis Controls Gene Expression

We demonstrated that PAIP2A was rapidly degraded by calpains in cultured neurons following stimulation with KCl and NMDA, in hippocampal slices after tetanic stimulation (TBS), and in vivo in the dorsal hippocampus after behavioral learning. It is interesting that PAIP2A levels returned to baseline within 30 min, showing that PAIP2A levels are dynamically controlled by a steady-state balance between protein synthesis and degradation by calpains. Calpains are ubiquitously expressed, calcium-activated, intracellular cysteine proteases that play important roles in synaptic plasticity, memory, and neurodegeneration (Wu and Lynch, 2006; Zadran et al., 2010). In neurons, calpains are activated by calcium influx following NMDA receptor activation and TBS (Vanderklish et al., 1995, 2000), and inhibition of calpain activity suppresses L-LTP (Denny et al., 1990; Staubli et al., 1988; Vanderklish et al., 1996) and memory (Lynch and

Figure 7. Facilitation of Activity-Dependent CaMKIIα Expression in Slices from *Paip2a*$^{-/-}$ Mice

(A–C) Hippocampal slices, with surgical cut across CA1 layers to isolate tetanized and untetanized regions, were stimulated with an electrode placed in the middle of stratum radiatum proximal to CA3 (marked by white circle). Slices from WT and *Paip2a*$^{-/-}$ mice were stimulated with either 1HFS or TBS and 30 min later were fixed and immunostained for CaMKIIα. fEPSPs were recorded at 0.033 Hz 10 min before and 30 min after tetanization to verify LTP induction. Activity-dependent dendritic expression of CaMKIIα was assessed by measuring mean fluorescent signal intensity in the areas located ~100 μm from the lesion in the middle of the stratum radiatum. The ratio of signal from stimulated (black square) to unstimulated (white square) regions reflects stimulation-induced dendritic expression of CaMKIIα. The signal in the cell body layer (stratum pyramidale) was measured in the corresponding area. 1HFS induces no increase in CaMKIIα signal in WT slices (A), whereas it leads to CaMKIIα upregulation in *Paip2a*$^{-/-}$ slices (B). Anisomycin (50 μM) applied 30 min before and during tetanization completely blocked CaMKIIα upregulation (C).

(D) Quantification of the results after normalization to the ratio obtained from untetanized WT and KO slices.

(E) Quantification of CaMKIIα ratio at 30 min after TBS in WT and *Paip2a*$^{-/-}$ slices. Data are presented as mean ± SEM. *$p < 0.05$.

(F) Reduction of PABP protein levels decreases LTM of *Paip2a*$^{-/-}$ mice. WT and *Paip2a*$^{-/-}$ mice, injected into the dorsal hippocampus with the lentiviruses expressing shRNA against *PABP* or nontargeting sequence, were subjected to the contextual fear conditioning (using weak training protocol) 7 days later. Western blot analysis of lysates from the dorsal hippocampus confirmed reduction of PABP protein levels.

(G) Behavioral experiments showed that the enhanced freezing measured 24 hr after the training of *Paip2a*$^{-/-}$ mice (injected with the control shRNA) was reduced in *Paip2a*$^{-/-}$ mice injected with shRNA against PABP ($n = 8$ per group, $p < 0.05$).

(H) A model for regulation of long-term synaptic plasticity and memory formation via proteolysis of PAIP2A by calpains. Neuronal stimulation leads to calcium entry and calpain activation that, in turn, degrades PAIP2A. A decreased PAIP2A allows PABP to bind poly(A) tail of mRNAs, resulting in enhanced translation. mRNAs containing CPE, such as CaMKIIα are preferably translated due to both activity-dependent poly(A) tail elongation and PAIP2A degradation.

Baudry, 1984; Shimizu et al., 2007; Zadran et al., 2010). Previous work has identified a suprachiasmatic nucleus circadian oscillatory protein (SCOP) as a calpain substrate, whose activity-dependent degradation stimulates mitogen-activated protein kinase (MAPK) signaling and transcription mediated by cAMP response element-binding protein (Shimizu et al., 2007). Mice overexpressing SCOP exhibited impaired long-term memory for novel objects, suggesting that SCOP degradation contributes to memory formation via MAPK activation. It is interesting that, in the mammalian brain, MAPK activity regulates mRNA translation and memory (Kelleher et al., 2004b). Our data indicate that, in addition to SCOP, calpains control synaptic plasticity and memory, in part via activity-dependent degradation of PAIP2A. Despite the similarity in the mechanisms of activity-dependent regulation of SCOP and PAIP2A levels in the brain, their downstream effectors are different; therefore, memory alterations in *Paip2a*$^{-/-}$ and SCOP-overexpressing mice are not similar. SCOP-overexpressing mice exhibit impaired novel object recognition LTM (Shimizu et al., 2007), while PAIP2A deletion results in alterations in contextual fear and spatial LTM.

The Threshold for Both L-LTP Induction and CaMKIIα Translation Is Lowered in *Paip2a*$^{-/-}$ Mice

We showed here that, in *Paip2a*$^{-/-}$ mice, the threshold for induction of the protein synthesis-dependent phase of LTP is lowered, and L-LTP was induced with just 1HFS. Remarkably, the threshold for the induction of CaMKIIα translation was similarly reduced in slices from *Paip2a*$^{-/-}$ mice. 1HFS in *Paip2a*$^{-/-}$ slices induced robust CaMKIIα expression, whereas no significant CaMKIIα expression was observed in WT slices. This indicates that the threshold for induction of L-LTP is determined by the sensitivity of the translational machinery to stimulation, which is negatively controlled by PAIP2A.

Strong Stimulation in *Paip2a*$^{-/-}$ Mice Leads to Excessive mRNA Translation and L-LTP and Memory Deficits

Long-term memory in *Paip2a*$^{-/-}$ mice was enhanced after weak training, paralleling the low threshold for induction of L-LTP and translation. In response to more intense stimulation (TBS or strong contextual fear conditioning), L-LTP and LTM were impaired, akin to earlier reports using other suppressors of translation, such as 4E-BP2 and GCN2 (Banko et al., 2005; Costa-Mattioli et al., 2005). Similar to *Paip2a*$^{-/-}$, in 4E-BP2 and GCN2$^{-/-}$ hippocampal slices 1HFS elicited L-LTP, while stronger tetanic stimulation (4HFS) led to L-LTP impairment. Moreover, weak training enhanced LTM in GCN2$^{-/-}$ mice, while more intense training caused LTM deficits. In *Tsc2*$^{+/-}$ mice, the mTOR pathway, an important regulator of translation, is hyperactivated resulting in impaired memory (Ehninger et al., 2008). Treatment with the mTOR inhibitor, rapamycin, reversed the learning and memory deficits, indicating that enhanced mTOR activity—and probably translation—are responsible for memory deficits (Ehninger et al., 2008). A conceivable explanation for the impairment is that strong stimulation in *Paip2a*$^{-/-}$ mice results in excessive translation leading to impairment of L-LTP and memory. One possibility is that synthesis of proteins detrimental to L-LTP and memory maintenance (negative regulators) after strong stimulation in *Paip2a*$^{-/-}$ mice leads to L-LTP and memory deficits. Physiologically, this mechanism can serve to protect the brain under conditions of excessive stimulation such as seizure activity. Alternatively, enhanced activity-dependent translation could induce uncoordinated neuronal activity that might lead to L-LTP and memory impairment. In support of our model, we showed that in the contextual fear conditioning task strong training of *Paip2a*$^{+/-}$ mice, in which the PAIP2A level is reduced by half, resulted in enhancement of LTM, conceivably because the activity-induced translation is enhanced to a lower extent that does not lead to L-LTP and memory deficits.

In summary, we have uncovered a mechanism for activity-dependent regulation of mRNA translation in the mammalian brain through the control of PABP activity by the PABP-binding protein PAIP2A. We show that degradation of PAIP2A by calpains releases PABP from inhibitory PAIP2-PABP complexes thereby enhancing PABP binding to memory-related mRNAs and stimulating their translation. Thus, PAIP2A is a negative translational regulator of mammalian synaptic plasticity and memory.

EXPERIMENTAL PROCEDURES

Paip2a and Paip2b KO Mice

Paip2a$^{-/-}$ and *Paip2b*$^{-/-}$ mice (Yanagiya et al., 2010) were backcrossed for more than 10 generations to C57BL/6J mice. For all behavioral tasks, 8- to 12-week-old *Paip2a*$^{-/-}$ and *Paip2b*$^{-/-}$ and their male WT littermates were used. The experimenter was blind to the genotype in all studies. Food and water were provided ad libitum, and mice were kept on a 12:12 hr light/dark cycle (lights on at 08:00 hr). All procedures complied with Canadian Council on Animal Care guidelines and were approved by Université de Montréal's and McGill University's animal care committees.

Electrophysiology

Transverse hippocampal slices (400 μm), prepared from WT or *Paip2a*$^{-/-}$ male littermates (6–8 weeks old), were allowed to recover submerged for at least 2 hr at 32°C in oxygenated artificial cerebrospinal fluid (ACSF) containing 124 mM NaCl, 2.5 mM KCl, 1.25 mM NaH_2PO_4, 1.3 mM $MgSO_4$, 2.5 mM $CaCl_2$, 26 mM $NaHCO_3$ and 10 mM glucose, and for an additional 30 min submerged in a recording chamber at 27°C–28°C while continuously perfused with ACSF. fEPSPs were recorded in CA1 stratum radiatum with glass electrodes (2–3 MΩ) filled with ASCF. Schaffer collateral fEPSPs were evoked by stimulation with a concentric bipolar tungsten stimulating electrode placed in midstratum radiatum proximal to CA3 region. For two-pathway experiments, two stimulating electrodes were placed in the proximal and distal CA1 stratum radiatum on either side of the recording electrode. The independence between pathways was verified at the onset of every experiment. Baseline stimulation was applied at 0.033 Hz by delivering 0.1 ms pulses, with intensity adjusted to evoke 35% of maximal fEPSPs. To induce LTP with tetanic stimulation, a single train was delivered at 100 Hz for 1 s. TBS consisted of 15 bursts of four pulses at 100 Hz separated by 200 ms intervals. DHPG (50 μM, Tocris) was added to ACSF for 10 min to induce mGluR-mediated LTD. To induce NMDA-receptor-mediated LTD with LFS, 900 pulses at 1 Hz were delivered. Slices used for LFS-induced LTD were allowed to recover for at least 4 hr before the experiment. Anisomycin (40 μM), actinomycin-D (40 μM), or calpeptin (10 μM), all from Calbiochem, were applied 30 min before the onset and during tetanic stimulation. The experiments were performed by researchers blind to the mouse genotype. Statistical analyses were done by Student's t tests and one-way ANOVA. All data are presented as means ± SEM, and n indicates the number of slices.

Western Blotting, Immunoprecipitation, and Oligo(dt) Pull-Down Assay

Proteins were resolved on SDS-polyacrylamide gels using standard techniques. See Supplemental Experimental Procedures for details of the Experimental Procedures and antibodies used.

RIP Assay

Dorsal hippocampi were homogenized in immunoprecipitation buffer containing RNase inhibitors (Rnasin, Promega), as described previously for immunoprecipitation. To immobilize the PABP antibody to beads, Dynabeads Protein G (Invitrogen) were incubated with 5 μg of PABP antibody (Catalog ab21060, Abcam) or rabbit preimmune serum at 4°C for 2 hr and then washed four times to remove the unbound antibody. After preclearing, equal amounts of lysate were incubated with the beads at 4°C for 2 hr. Following four washes, RNA was extracted from the beads using TRIzol (Invitrogen). Reverse transcription was performed using a SuperScript III Reverse-Transcriptase Kit (Invitrogen) according to the manufacturer's instructions. qRT-PCRs were carried out using iQ Sybr Green Supermix (Bio-Rad) according to the manufacturer's instructions, and the results were normalized to the values obtained with rabbit preimmune serum.

MWM

The water pool was 100 cm in diameter, and the platform was 10 cm in diameter. Water was kept at 24°C. Mice were handled daily for 3 days before the experiment and trained with one trial per day protocol. Each mouse swam until it found the hidden platform. If the mouse had not found the platform after 120 s, it was gently guided to the platform and stayed there for 10 s before being returned to the cage. For the probe test, the platform was removed and each mouse was allowed to swim for 60 s. The swimming trajectory was monitored with a video tracking system (HVS Image).

Contextual and Auditory Fear Conditioning, Object Location, and Novel Object Recognition Tasks

Contextual and auditory fear conditioning experiments were performed as previously described (Costa-Mattioli et al., 2007). See Supplemental Experimental Procedures for details.

Dissociated Neuronal Culture

Cortices from E16-E18 C57BL/6 embryos were used for the preparation of dissociated neuronal culture. See Supplemental Experimental Procedures for details.

Synaptosome Preparation

Intact hippocampi from C57BL/6 mice were dissected and homogenized in 320 mM sucrose, 1 mM EDTA, 5 mM Tris-HCl (pH 7.4), and 25 μM dithiothreitol. Synaptosomes were isolated on a discontinuous Percoll (GE Healthcare) gradient. The fraction between 15% and 23% Percoll was isolated and resuspended in SDS-PAGE buffer.

Immunohistochemistry

The procedures for fluorescent immunostaining and data analysis were previously described (Gong et al., 2006). For more details and the procedure for image acquisition and analysis, see Supplemental Experimental Procedures.

Polysome Profile Analysis and qRT-PCR

The experimental procedure for polysome profiling was performed as in (Parsyan et al., 2009) with minor modifications. See Supplemental Experimental Procedures for more details.

Statistical Analysis

All results are expressed as mean ± SEM. All statistical comparisons were made with either the Student's t test or a one-way ANOVA followed by between-group comparisons using Tukey's post hoc test, unless otherwise indicated, with $p < 0.05$ as significance criterion.

SUPPLEMENTAL INFORMATION

Supplemental Information includes five figures and Supplemental Experimental Procedures and can be found with this article online at http://dx.doi.org/10.1016/j.neuron.2013.02.025.

ACKNOWLEDGMENTS

We thank Wayne Sossin and Valerie Henderson for excellent comments; Annie Sylvestre, Sandra Perreault, and Colin Lister for technical assistance; and Isabel Laplante for assistance with immunostaining. This work was supported by National Institutes of Health Grant 2R01GM066157 and a Canadian Institutes of Health Research (CIHR) grant to Nahum Sonenberg and CIHR Grant MOP-10848 to J.C.L. J.C.L. is the recipient of the Canada Research Chair in Cellular and Molecular Neurophysiology.

Accepted: February 22, 2013
Published: April 24, 2013

REFERENCES

Aakalu, G., Smith, W.B., Nguyen, N., Jiang, C., and Schuman, E.M. (2001). Dynamic visualization of local protein synthesis in hippocampal neurons. Neuron *30*, 489–502.

Abel, T., Martin, K.C., Bartsch, D., and Kandel, E.R. (1998). Memory suppressor genes: inhibitory constraints on the storage of long-term memory. Science *279*, 338–341.

Assini, F.L., Duzzioni, M., and Takahashi, R.N. (2009). Object location memory in mice: pharmacological validation and further evidence of hippocampal CA1 participation. Behav. Brain Res. *204*, 206–211.

Banerjee, S., Neveu, P., and Kosik, K.S. (2009). A coordinated local translational control point at the synapse involving relief from silencing and MOV10 degradation. Neuron *64*, 871–884.

Banko, J.L., Poulin, F., Hou, L., DeMaria, C.T., Sonenberg, N., and Klann, E. (2005). The translation repressor 4E-BP2 is critical for eIF4F complex formation, synaptic plasticity, and memory in the hippocampus. J. Neurosci. *25*, 9581–9590.

Berlanga, J.J., Baass, A., and Sonenberg, N. (2006). Regulation of poly(A) binding protein function in translation: Characterization of the Paip2 homolog, Paip2B. RNA *12*, 1556–1568.

Bhattacharya, A., Kaphzan, H., Alvarez-Dieppa, A.C., Murphy, J.P., Pierre, P., and Klann, E. (2012). Genetic removal of p70 S6 kinase 1 corrects molecular, synaptic, and behavioral phenotypes in fragile X syndrome mice. Neuron *76*, 325–337.

Bingol, B., and Schuman, E.M. (2006). Activity-dependent dynamics and sequestration of proteasomes in dendritic spines. Nature *441*, 1144–1148.

Bingol, B., and Sheng, M. (2011). Deconstruction for reconstruction: the role of proteolysis in neural plasticity and disease. Neuron *69*, 22–32.

Burgin, K.E., Waxham, M.N., Rickling, S., Westgate, S.A., Mobley, W.C., and Kelly, P.T. (1990). In situ hybridization histochemistry of Ca2+/calmodulin-dependent protein kinase in developing rat brain. J. Neurosci. *10*, 1788–1798.

Chan, S.L., and Mattson, M.P. (1999). Caspase and calpain substrates: roles in synaptic plasticity and cell death. J. Neurosci. Res. *58*, 167–190.

Costa-Mattioli, M., Gobert, D., Harding, H., Herdy, B., Azzi, M., Bruno, M., Bidinosti, M., Ben Mamou, C., Marcinkiewicz, E., Yoshida, M., et al. (2005). Translational control of hippocampal synaptic plasticity and memory by the eIF2alpha kinase GCN2. Nature *436*, 1166–1173.

Costa-Mattioli, M., Gobert, D., Stern, E., Gamache, K., Colina, R., Cuello, C., Sossin, W., Kaufman, R., Pelletier, J., Rosenblum, K., et al. (2007). eIF2alpha phosphorylation bidirectionally regulates the switch from short- to long-term synaptic plasticity and memory. Cell *129*, 195–206.

del Cerro, S., Larson, J., Oliver, M.W., and Lynch, G. (1990). Development of hippocampal long-term potentiation is reduced by recently introduced calpain inhibitors. Brain Res. *530*, 91–95.

Denny, J.B., Polan-Curtain, J., Ghuman, A., Wayner, M.J., and Armstrong, D.L. (1990). Calpain inhibitors block long-term potentiation. Brain Res. *534*, 317–320.

Derry, M.C., Yanagiya, A., Martineau, Y., and Sonenberg, N. (2006). Regulation of poly(A)-binding protein through PABP-interacting proteins. Cold Spring Harb. Symp. Quant. Biol. *71*, 537–543.

Ehninger, D., Han, S., Shilyansky, C., Zhou, Y., Li, W., Kwiatkowski, D.J., Ramesh, V., and Silva, A.J. (2008). Reversal of learning deficits in a Tsc2+/- mouse model of tuberous sclerosis. Nat. Med. *14*, 843–848.

Frankland, P.W., O'Brien, C., Ohno, M., Kirkwood, A., and Silva, A.J. (2001). Alpha-CaMKII-dependent plasticity in the cortex is required for permanent memory. Nature *411*, 309–313.

Giese, K.P., Fedorov, N.B., Filipkowski, R.K., and Silva, A.J. (1998). Autophosphorylation at Thr286 of the alpha calcium-calmodulin kinase II in LTP and learning. Science *279*, 870–873.

Gong, R., Park, C.S., Abbassi, N.R., and Tang, S.J. (2006). Roles of glutamate receptors and the mammalian target of rapamycin (mTOR) signaling pathway in activity-dependent dendritic protein synthesis in hippocampal neurons. J. Biol. Chem. *281*, 18802–18815.

Gray, N.K., Coller, J.M., Dickson, K.S., and Wickens, M. (2000). Multiple portions of poly(A)-binding protein stimulate translation in vivo. EMBO J. *19*, 4723–4733.

Hoeffer, C.A., Tang, W., Wong, H., Santillan, A., Patterson, R.J., Martinez, L.A., Tejada-Simon, M.V., Paylor, R., Hamilton, S.L., and Klann, E. (2008). Removal of FKBP12 enhances mTOR-Raptor interactions, LTP, memory, and perseverative/repetitive behavior. Neuron *60*, 832–845.

Hoeffer, C.A., Cowansage, K.K., Arnold, E.C., Banko, J.L., Moerke, N.J., Rodriguez, R., Schmidt, E.K., Klosi, E., Chorev, M., Lloyd, R.E., et al. (2011). Inhibition of the interactions between eukaryotic initiation factors 4E and 4G impairs long-term associative memory consolidation but not reconsolidation. Proc. Natl. Acad. Sci. USA *108*, 3383–3388.

Huang, Y.S., Jung, M.Y., Sarkissian, M., and Richter, J.D. (2002). N-methyl-D-aspartate receptor signaling results in Aurora kinase-catalyzed CPEB phosphorylation and alpha CaMKII mRNA polyadenylation at synapses. EMBO J. *21*, 2139–2148.

Kahvejian, A., Roy, G., and Sonenberg, N. (2001). The mRNA closed-loop model: the function of PABP and PABP-interacting proteins in mRNA translation. Cold Spring Harb. Symp. Quant. Biol. *66*, 293–300.

Kandel, E.R. (2001). The molecular biology of memory storage: a dialogue between genes and synapses. Science *294*, 1030–1038.

Karim, M.M., Svitkin, Y.V., Kahvejian, A., De Crescenzo, G., Costa-Mattioli, M., and Sonenberg, N. (2006). A mechanism of translational repression by competition of Paip2 with eIF4G for poly(A) binding protein (PABP) binding. Proc. Natl. Acad. Sci. USA *103*, 9494–9499.

Kelleher, R.J., 3rd, Govindarajan, A., and Tonegawa, S. (2004a). Translational regulatory mechanisms in persistent forms of synaptic plasticity. Neuron *44*, 59–73.

Kelleher, R.J., 3rd, Govindarajan, A., Jung, H.Y., Kang, H., and Tonegawa, S. (2004b). Translational control by MAPK signaling in long-term synaptic plasticity and memory. Cell *116*, 467–479.

Khaleghpour, K., Svitkin, Y.V., Craig, A.W., DeMaria, C.T., Deo, R.C., Burley, S.K., and Sonenberg, N. (2001). Translational repression by a novel partner of human poly(A) binding protein, Paip2. Mol. Cell *7*, 205–216.

Li, Z., Jo, J., Jia, J.M., Lo, S.C., Whitcomb, D.J., Jiao, S., Cho, K., and Sheng, M. (2010). Caspase-3 activation via mitochondria is required for long-term depression and AMPA receptor internalization. Cell *141*, 859–871.

Lonergan, M.E., Gafford, G.M., Jarome, T.J., and Helmstetter, F.J. (2010). Time-dependent expression of Arc and zif268 after acquisition of fear conditioning. Neural Plast. *2010*, 139891.

Lynch, G., and Baudry, M. (1984). The biochemistry of memory: a new and specific hypothesis. Science *224*, 1057–1063.

Lynch, G., Rex, C.S., and Gall, C.M. (2007). LTP consolidation: substrates, explanatory power, and functional significance. Neuropharmacology *52*, 12–23.

Martineau, Y., Derry, M.C., Wang, X., Yanagiya, A., Berlanga, J.J., Shyu, A.B., Imataka, H., Gehring, K., and Sonenberg, N. (2008). Poly(A)-binding protein-interacting protein 1 binds to eukaryotic translation initiation factor 3 to stimulate translation. Mol. Cell. Biol. *28*, 6658–6667.

Mayford, M., Baranes, D., Podsypanina, K., and Kandel, E.R. (1996a). The 3′-untranslated region of CaMKII alpha is a cis-acting signal for the localization and translation of mRNA in dendrites. Proc. Natl. Acad. Sci. USA *93*, 13250–13255.

Mayford, M., Bach, M.E., Huang, Y.Y., Wang, L., Hawkins, R.D., and Kandel, E.R. (1996b). Control of memory formation through regulated expression of a CaMKII transgene. Science *274*, 1678–1683.

Miller, S., Yasuda, M., Coats, J.K., Jones, Y., Martone, M.E., and Mayford, M. (2002). Disruption of dendritic translation of CaMKIIalpha impairs stabilization of synaptic plasticity and memory consolidation. Neuron *36*, 507–519.

Morris, R.G., Garrud, P., Rawlins, J.N., and O'Keefe, J. (1982). Place navigation impaired in rats with hippocampal lesions. Nature *297*, 681–683.

Muddashetty, R., Khanam, T., Kondrashov, A., Bundman, M., Iacoangeli, A., Kremerskothen, J., Duning, K., Barnekow, A., Hüttenhofer, A., Tiedge, H., and Brosius, J. (2002). Poly(A)-binding protein is associated with neuronal BC1 and BC200 ribonucleoprotein particles. J. Mol. Biol. *321*, 433–445.

Ouyang, Y., Rosenstein, A., Kreiman, G., Schuman, E.M., and Kennedy, M.B. (1999). Tetanic stimulation leads to increased accumulation of Ca(2+)/calmodulin-dependent protein kinase II via dendritic protein synthesis in hippocampal neurons. J. Neurosci. *19*, 7823–7833.

Pan, Y.W., Chan, G.C., Kuo, C.T., Storm, D.R., and Xia, Z. (2012). Inhibition of adult neurogenesis by inducible and targeted deletion of ERK5 mitogen-activated protein kinase specifically in adult neurogenic regions impairs contextual fear extinction and remote fear memory. J. Neurosci. *32*, 6444–6455.

Parsyan, A., Shahbazian, D., Martineau, Y., Petroulakis, E., Alain, T., Larsson, O., Mathonnet, G., Tettweiler, G., Hellen, C.U., Pestova, T.V., et al. (2009). The helicase protein DHX29 promotes translation initiation, cell proliferation, and tumorigenesis. Proc. Natl. Acad. Sci. USA *106*, 22217–22222.

Richter, J.D., and Klann, E. (2009). Making synaptic plasticity and memory last: mechanisms of translational regulation. Genes Dev. *23*, 1–11.

Shimizu, K., Phan, T., Mansuy, I.M., and Storm, D.R. (2007). Proteolytic degradation of SCOP in the hippocampus contributes to activation of MAP kinase and memory. Cell *128*, 1219–1229.

Silva, A.J. (2003). Molecular and cellular cognitive studies of the role of synaptic plasticity in memory. J. Neurobiol. *54*, 224–237.

Silva, A.J., Paylor, R., Wehner, J.M., and Tonegawa, S. (1992a). Impaired spatial learning in alpha-calcium-calmodulin kinase II mutant mice. Science *257*, 206–211.

Silva, A.J., Stevens, C.F., Tonegawa, S., and Wang, Y. (1992b). Deficient hippocampal long-term potentiation in alpha-calcium-calmodulin kinase II mutant mice. Science *257*, 201–206.

Staubli, U., Larson, J., Thibault, O., Baudry, M., and Lynch, G. (1988). Chronic administration of a thiol-proteinase inhibitor blocks long-term potentiation of synaptic responses. Brain Res. *444*, 153–158.

Sutton, M.A., and Schuman, E.M. (2006). Dendritic protein synthesis, synaptic plasticity, and memory. Cell *127*, 49–58.

Vanderklish, P., Saido, T.C., Gall, C., Arai, A., and Lynch, G. (1995). Proteolysis of spectrin by calpain accompanies theta-burst stimulation in cultured hippocampal slices. Brain Res. Mol. Brain Res. *32*, 25–35.

Vanderklish, P., Bednarski, E., and Lynch, G. (1996). Translational suppression of calpain blocks long-term potentiation. Learn. Mem. *3*, 209–217.

Vanderklish, P.W., Krushel, L.A., Holst, B.H., Gally, J.A., Crossin, K.L., and Edelman, G.M. (2000). Marking synaptic activity in dendritic spines with a calpain substrate exhibiting fluorescence resonance energy transfer. Proc. Natl. Acad. Sci. USA *97*, 2253–2258.

Wu, H.Y., and Lynch, D.R. (2006). Calpain and synaptic function. Mol. Neurobiol. *33*, 215–236.

Wu, L., Wells, D., Tay, J., Mendis, D., Abbott, M.A., Barnitt, A., Quinlan, E., Heynen, A., Fallon, J.R., and Richter, J.D. (1998). CPEB-mediated cytoplasmic polyadenylation and the regulation of experience-dependent translation of alpha-CaMKII mRNA at synapses. Neuron *21*, 1129–1139.

Yanagiya, A., Delbes, G., Svitkin, Y.V., Robaire, B., and Sonenberg, N. (2010). The poly(A)-binding protein partner Paip2a controls translation during late spermiogenesis in mice. J. Clin. Invest. *120*, 3389–3400.

Yoshida, M., Yoshida, K., Kozlov, G., Lim, N.S., De Crescenzo, G., Pang, Z., Berlanga, J.J., Kahvejian, A., Gehring, K., Wing, S.S., and Sonenberg, N. (2006). Poly(A) binding protein (PABP) homeostasis is mediated by the stability of its inhibitor, Paip2. EMBO J. *25*, 1934–1944.

Zadran, S., Bi, X., and Baudry, M. (2010). Regulation of calpain-2 in neurons: implications for synaptic plasticity. Mol. Neurobiol. *42*, 143–150.